ELSEVIER

PII: S0032-3861(97)10132-X

Polymer Vol. 39 No. 19, pp. 4593–4598, 1998

0032-3861/98/$19.00+0.00

Effects of crystalline forms on the deformation behaviour of nylon-6

Masayoshi Ito[a,*], Kazuko Mizuochi[a] and Tetsuo Kanamoto[b]
[a]*Department of Chemistry, Science University of Tokyo, Kagurazaka, Shinjuku-ku, Tokyo 162, Japan*
[b]*Department of Applied Chemistry, Science University of Tokyo, Kagurazaka, Shinjuku-ku, Tokyo 162, Japan*
(Received 29 May 1997; revised 11 August 1997; accepted 12 August 1997)

Solid-state coextrusion draw was carried out for films of aggregates of solution- and melt-grown crystals of nylon-6 with α- and γ-forms. Under ordinal crystallization conditions, the crystal form was primarily a monoclinic α-form. Thus, α-crystals were converted to the γ-form by iodine treatment, followed by treatment with aqueous solution of sodium thiosulfate. The maximum extrusion draw ratio achieved (EDR_{max}) at temperatures in the range of 100–180°C was greatly affected by both the crystal forms and the initial morphologies. At a given crystal morphology, the EDR_{max} for the γ-crystals was higher than the α-crystals. Further, the efficiency of draw evaluated from the crystalline chain orientation was higher for γ-crystals than α-crystals. For films with α-cry6 the intercrystalline network has an important role in transmitting the stress on draw. On the other hand, for films with γ-crystals, the effect of intercrystalline network on the efficiency of draw was less prominent. These results were almost independent of the extrusion temperature studied. The effect of crystal form on the ductility is explained based on the difference in the interchain interactions due to hydrogen bonding in the crystalline regions.

(Keywords: nylon-6; crystalline form; deformation)

INTRODUCTION

Extensive work on the deformation of nonpolar semicrystalline polymers has established that the entanglement density is one of the crucial factors determining the ductility of polymers[1–4]. We have shown that an effect of entanglements was also applicable to polar polymers including poly(ethylene terephthalate)[5]. Further, Lin and Argon[6] reported that the interchain interactions, such as hydrogen bonding, suppress the shear slip of the crystalline chains during deformation. The ductility of polymers is primarily determined by the competition between the shear deformation resistance and the tensile strength of the samples. Thus, a systematic study is necessary for the understanding of the effects of interchain interactions on the deformation mechanism of semicrystalline polymers.

Nylon-6 crystals can exist in two major forms; monoclinic α-form and monoclinic or pseudo hexagonal γ-form[7–9]. The principal difference between the two forms is a molecular packing. In the α-form, hydrogen bondings are formed between antiparallel chains. In the γ-form, molecular chains have to twist away from the zigzag planes to form hydrogen bonding between parallel chains. As a result, the crystal density for the γ-form is smaller than that for the α-form. In addition, the distance between adjacent amidic groups, where hydrogen bondings are formed, is longer for the γ-form than for α-form. These results suggest that interchain interactions in the γ-form is smaller than the α-form. Thus, the deformation behaviour of the two crystalline forms may give useful information on the effect of interchain interaction on the ductility of semicrystalline polymers.

In this study, solid-state coextrusion was carried out for films of aggregates of solution- and melt-grown crystals of nylon-6 with α-and γ-forms. The solution-grown crystals were composed of lamellar crystals with a minimum number of intervening tie chains and entanglements. Such a relatively simple structure is suitable for the evaluation of the deformation mechanism of semicrystalline polymers with strong interchain interactions.

Under ordinal crystallization conditions, the crystalline form of both solution- and melt-grown crystals of nylon-6 is a monoclinic α-form. Thus, α-crystals were converted to the γ-form by iodine treatment[10]. The predominant mechanism for the morphological transformation of lamellae to a fibrous structure is discussed in relation to the interchain interactions of crystalline phases by comparing the deformation behaviour of α-crystals with that of γ-crystals.

EXPERIMENTAL

Sample preparation

Nylon-6 (intrinsic viscosity = 1.0 dl/g) was kindly supplied by Toyobo, as polymer chips, free of additives. The chips were dissolved in hexylene glycol at 190°C, and solutions containing 0.07 wt.% of polymer were prepared. The crystals were precipitated from solution during slow cooling from 190°C to room temperature. Oriented films of solution-grown crystals (SGC film) were prepared by slowly filtering the crystal suspension at room temperature. The wet films were washed with methanol to exchange hexylene glycol with a more volatile solvent, then they were dried at 40°C for 12 h under vacuum. Films of melt-grown crystals (MGC film) were obtained by a compression

* To whom correspondence should be addressed

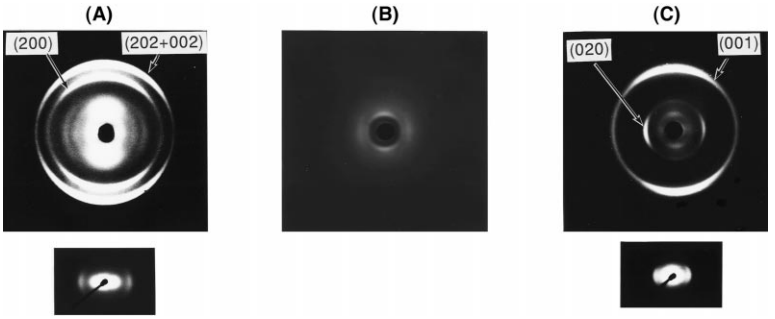

Figure 1 WAXD and SAXS photographs of the original SGC film (A), iodine-treated film (B), and sodium thiosulfate-treated (reduced) film (C)

molding of the polymer chips at 240°C, followed by slow cooling to room temperature. The SGC and MGC films of ~0.1 mm thickness were immersed in an iodine–potassium aqueous solution for 168 h at room temperature. The aqueous solution was composed of 39 g of iodine, 47 g of potassium iodide and 300 cc of distilled water. The iodine was washed out from the films by keeping them in a 0.13-mol/l sodium thiosulfate solution for 120 h at 25°C. After the treatment of wash solution, no trace of iodine was detected in the films by elemental analysis.

Melt-crystallized polyethylene or poly(4-methyl-1-pentene) billets were cut in half, the SGC and MGC films were then placed between the halves of the split billets, and the assembly was coextruded at a constant temperature in the range of 100–180°C. The extrusion draw ratio (EDR) was evaluated by a measuring the separation between lateral ink marks on the samples before and after the coextrusion.

Measurements

Wide-angle (WAXD) and small-angle X-ray scattering (SAXS) measurements were carried out on a Rigaku RU-200 diffraction unit with a Ni-filtered Cu Kα radiation generated at 50 kV and 150 mA. The longitudinal crystallite sizes were determined from $(0\ 14\ 0)_\alpha$ and $(0\ 2\ 0)_\gamma$ reflections for the α- and γ-forms, respectively, by using the Scherrer equation.

Sample densities were determined at 30°C in a density gradient column to an accuracy of $\pm$ 0.001 g/cm^3, using a mixture of *n*-heptane and carbon tetrachloride. The weight percent crystallinity was calculated from the observed density on the basis of a two-phase model. The crystalline densities were taken to be 1.24 and 1.16 g/cm^3 for the α-crystal[7] and the γ-crystal[10], respectively. The amorphous density was taken to be 1.08 g/cm^3[11].

The dynamic mechanical analyses were performed on a Rheovibron DDV-II-EP visco-elastometer (Orientec) at a frequency of 110 Hz. The measurements were carried out over a temperature range of 30–200°C at a heating rate of 1°C/min.

RESULTS AND DISCUSSION

Pre-drawn morphology

Figure 1 shows WAXD and SAXS photographs of the original SGC film (*Figure 1A*), the iodine-treated film (*Figure 1B*), followed by the sodium thiosulfate-treated film (reduced film, *Figure 1C*). These photographs were obtained with an incident X-ray beam parallel to the film surface. For the original film, the WAXD patterns showed that the crystals were predominantly in the α-form, and the intensity maxima of both the $(200)_\alpha$ and $(202 + 002)_\alpha$ reflections appeared on the meridian. The profiles suggest that the preferential orientation of the *b*-axis (the chain axis) is perpendicular to the film surface. In addition, the *a*- and *c*-axes are randomly oriented within the plane parallel to the film surface. In the SAXS patterns, the intensity maxima appeared on the equator, indicating the anisotropic orientation of lamellae with their fold surface parallel to the film surface. In this study, the direction of coextrusion was parallel to the surfaces of lamellae and SGC film. Thus at the initial stage of deformation, the averaged angle between the extrusion direction and the lamellar normal (ω) was about 90°. It was revealed in our previous paper[12], that the mechanism of morphological transformation from a lamellar to a fibrous structure during extrusion was almost independent of ω. The iodine-treated film showed no WAXD from the α-crystals and no SAXS maxima, suggesting that the sample was amorphous. Instead, weak but new diffraction arcs appeared at a low angle ($2\theta \simeq 12°$). Neither of these new peaks corresponds to the diffractions from the α- or γ-crystals. Several papers[13–17] report that the nylon-6 iodine complex has an unique structure characterized by three diffraction peaks at around $2\theta \simeq 5.3$, 11.5, and 23.0°. In this study, however, the details of the unique structure were not discussed, since such work was out of the scope of the present study.

The γ-form crystals appeared when the iodine molecules were eliminated by sodium thiosulfate and, simultaneously, the SAXS intensity maxima reappeared (*Figure 1C*). It is interesting that the direction of the crystal fiber axes in the γ-form is again perpendicular to the film surface, and that the fold surface of the lamellae is oriented parallel to the film surface, as observed for the initial SGC film. Such orientation is similar to that of the untreated original SGC film (see *Figure 1A*). After crystal conversion from α- to γ-form by the chemical treatments (reduced film), the long period as well as crystallite size along the chain direction were increased. Although the sample density decreased, the degrees of crystallinity were increased with chemical treatment, reflecting the lower crystal density of the γ-form compared with that of α-form. These are summarized in *Table 1*.

For the MGC film, the structural changes caused by the chemical treatments were slightly different from those observed in the SGC films. *Figure 2* shows WAXD and SAXS photographs of the original film (*Figure 2A*) and reduced film (*Figure 2B*). These photographs were obtained with the incident X-ray beam parallel to the film surface. The WAXD patterns of original film (*Figure 2A*) showed that the α-crystals oriented randomly within the film. After the iodine treatments, the α-crystals disappeared, similar to the case of SGC film (data not shown). With the sodium thiosulfate treatment (*Figure 2B*), γ-crystals with an

anisotropic orientation appeared. The degree of orientation increased with increasing the concentration of iodine molecules in the solutions (data not shown). At present, however, the reason for the appearance of an anisotropic arrangement of the crystals is not clear. Contrary to the case of the SGC film, the scattering intensity maxima in the SAXS profile were not reproduced by the sodium thiosulfate treatment. The missing intensity maxima in the SAXS profile of the reduced sample indicates that the difference in electron density between the crystalline and noncrystalline regions is small. Thus, the reduced sample was stained by RuO_4 vapor for 54 h, which selectively absorbed in the amorphous regions, leading to the observation of a long period of scattering maxima. The resultant SAXS patterns are shown in *Figure 3*. After the staining, the intensity maxima appeared with a slight anisotropic character. The long periods calculated from *Figure 3A* and *C* were 93 and 91 Å, respectively. Although, the change with chemical treatment is quite small compared with the case for the SGC samples, the value of 91 Å for the reduced sample is similar to that for the reduced SGC film. Unfortunately, for the original MGC film the reflection intensity from $(0\ 14\ 0)_\alpha$ plane was too weak to calculate the crystallite size. However, the longitudinal crystallite size of the reduced sample was 72 Å, comparable to that of the reduced SGC film. Further the degree of crystallinity for the MGC film increased from 46 to 68% with chemical treatments (see *Table 1*).

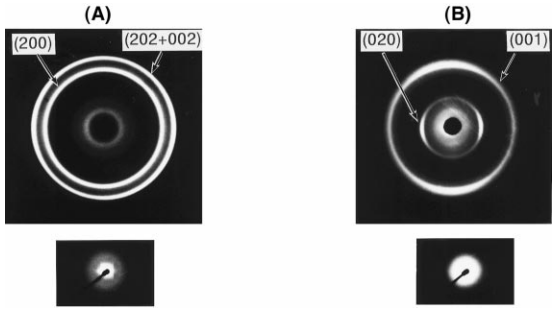

Figure 2 WAXD and SAXS photographs of the original MGC film (A) and the reduced film (B)

In order to evaluate the structural changes in noncrystalline regions with chemical treatments, dynamic mechanical measurements were carried out. *Figure 4* shows the temperature dependences of storage (E') and loss (E'') moduli for the original SGC and MGC films with α-crystals ($SGC_{(\alpha)}$ and $MGC_{(\alpha)}$) and the reduced SGC and MGC films with γ-crystals ($SGC_{(\gamma)}$ and $MGC_{(\gamma)}$). As can be seen in *Figures 1 and 2*, for the $SGC_{(\alpha)}$, $SGC_{(\gamma)}$ and $MGC_{(\gamma)}$, the molecular chains in the crystalline regions orient almost perpendicular to the film surface. In this work, the direction of dynamic stress was parallel to the film surface. Thus the data for the $SGC_{(\alpha)}$, $SGC_{(\gamma)}$ and $MGC_{(\gamma)}$ shown in *Figure 4* involved anisotropic characteristics. For the SGC films, both the original and reduced samples show, qualitatively, similar temperature dependences of E' and E''. At a given temperature, the two samples exhibited different values of E'. This arises because of the difference in the crystal modulus along the chain direction, since the crystal modulus of the γ-form is only 20% of that for the α-form in the original sample[18]. On the other hand, for the MGC films, the temperature dependences of E' and E'' for the reduced sample are quite different from those for the original sample. With the chemical treatments (reduced sample), the α-dispersion curve, corresponding to the onset of micro-Brownian motions of noncrystalline segments[19] became broader and shifted to a higher temperature. Simultaneously, the drop of E' around the α-dispersion became less prominent.

The results clearly indicate that the noncrystalline segments in the reduced film are highly strained, compared with those in the original film, suggesting that a large structural change was induced by the chemical treatments. The interesting fact is that the temperature dependences of E' and E'' for the MGC(γ) are similar to that of SGC(γ). As already mentioned, degrees of crystallinity, long period, and longitudinal crystallite size for the MGC(γ) are also similar to those for the SGC(γ). These results

Table 1 Structural factors of the original and reduced SGC and MGC films

Sample	Density (g/cm^3)	Crystallinity (%)	Long period (Å)	Crystal size (Å)[a]
SGC				
Original	1.166	58.7	64	45
Reduced	1.135	70.6	93	73
MGC				
Original	1.146	45.9	93	
Reduced	1.133	68.1	91	72

[a] Along the chain direction

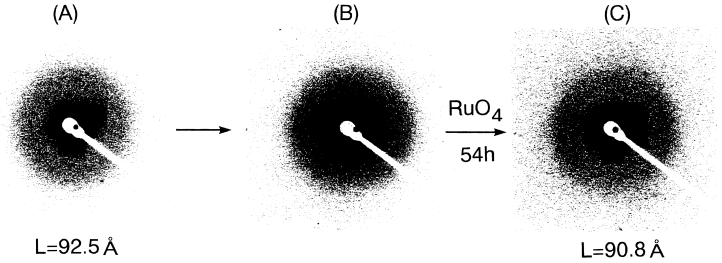

Figure 3 SAXS photographs of the original MGC film (A), reduced film (B), and the stained film (C)

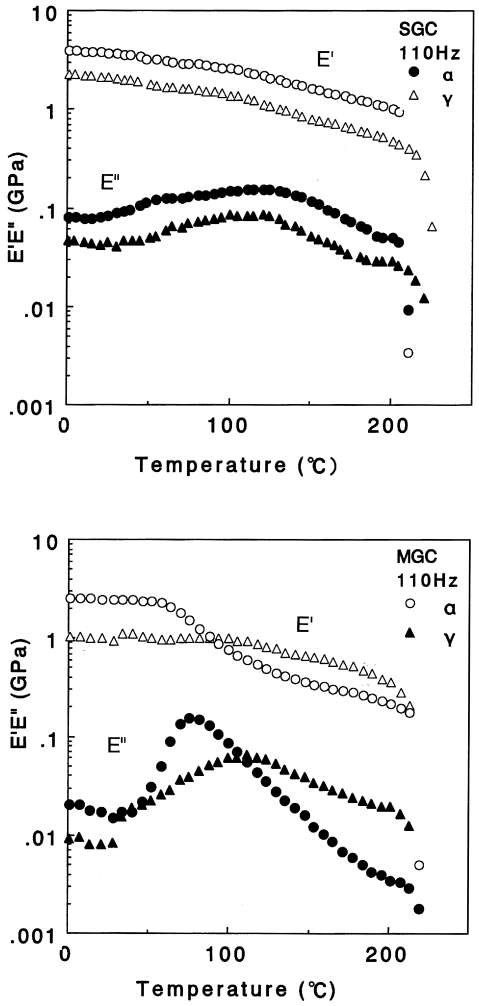

Figure 4 Temperature dependence of dynamic storage (E') and loss (E'') moduli for the SGC and MGC films with α- and γ-forms

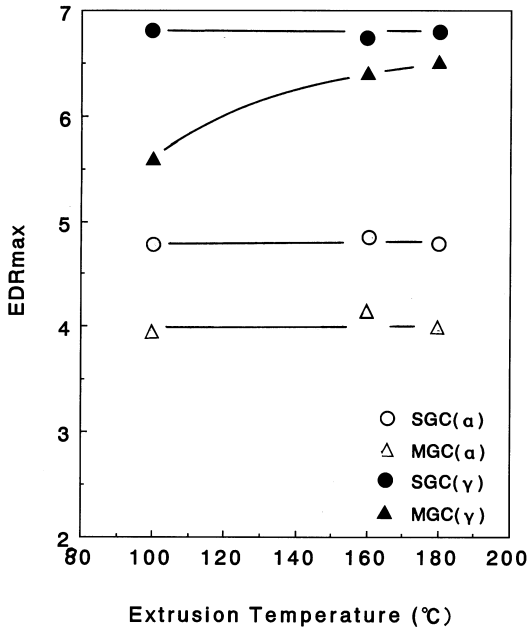

Figure 5 Relation between T_e and EDR_{max} for the SGC and MGC films with α- and γ-forms

suggest that the morphology of MGC(γ) is similar to that of SGC(γ).

Several mechanisms have been proposed for the transformation of the α- to the γ-form by iodine treatments, followed by the removal of iodine molecules with sodium thiosulfate[20–23]. The explanations, however, are sometimes controversial. As stated, the WAXD and SAXS results revealed that the iodine-treated SGC and MGC films were almost amorphous. When these amorphous films were treated with the aqueous solution of sodium thiosulfate, characteristic crystalline morphologies appeared in the treated films (reduced state). Further, the morphologies developed were dependent on the conditions for the treatments. With increasing treatment temperature and decreasing concentration of sodium thiosulfate in the solution, the fraction of α-crystals increased (data not shown). These results suggest that crystallization proceeds during the removal of iodine molecules by sodium thiosulfate from the amorphous films. The crystallization condition is a function of treatment temperature and the concentration of sodium thiosulfate. Therefore, the crystalline morphology developed in the reduced films is determined by the treatment conditions, independent of pretreated morphology. This consideration is partly supported by the experimental facts that MGC(γ) has a similar morphology to SGC(γ).

Deformation behaviour

In *Figure 5*, the maximum achieved extrusion draw ratio (EDR_{max}) is plotted against extrusion temperature (T_e) for $SGC_{(\alpha)}$, $SGC_{(\gamma)}$, $MGC_{(\alpha)}$ and $MGC_{(\gamma)}$ films. It can be seen that, for each set of SGC and MGC films, the EDR_{max} for the films with γ-crystals is higher than for films with α-crystals. In addition, for the same crystalline form, the EDR_{max} is higher for the SGC than for the MGC films. The results clearly indicate that the apparent ductility of nylon-6 crystals is higher for the γ-form than for the α-form. In addition, as has been observed in several polymers, the lower the entanglement density in the pre-drawn films, the higher the apparent ductility.

Numerous studies have been made of the deformation behaviour of nylon-6. However, most of them were limited to samples with α-crystals. Little work has been reported on the deformation mechanism of γ-crystals of nylon-6 and the morphological characteristics of the drawn fibers[23–26]. Arimoto reported[23] that the γ-crystals were destroyed and converted into the fiber structure of the usual α-form by drawing. On the other hand, Miyasaka and Ishikawa[24] suggest that the stress-induced γ to α conversion is a first-order crystal–crystal transition. However, none of the above mechanisms are correlated with the ductility of crystalline regions.

Figure 6 shows WAXD and SAXS photographs of the extrudates from the $SGC_{(\gamma)}$. The extrusion was made at 180°C. As can be seen in *Figure 5*, the $SGC_{(\gamma)}$ showed the highest EDR_{max} among the samples. At a small strain (EDR < 2), the intensity maxima in the WAXD profiles from the α-crystals appeared on the equator, but there still existed a strong intensity of reflection due to the γ-crystals keeping their initial orientation. The SAXS intensity maxima on the meridian became evident even at a small strain. At a larger strain (EDR > 4), the γ-crystals still exist, but the crystal fiber axes rotated from the original position to the extrusion direction. This means that a part of the γ-crystals cannot deform completely, even at the highest deformation ratio of 6.7 achieved in this work. At a higher EDR, the long period

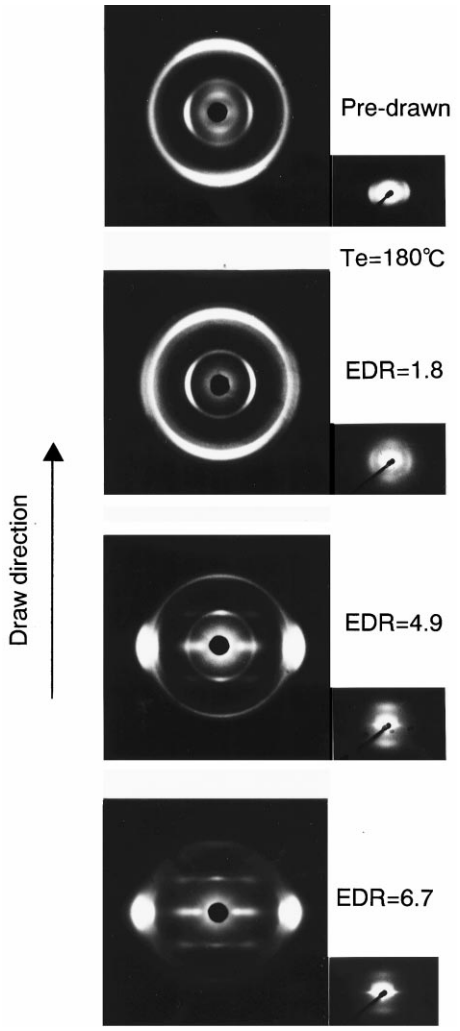

Figure 6 WAXD and SAXS photographs of the extrudates from $SGC_{(\gamma)}$ obtained at $T_e = 180°C$

along the fiber axis of the extrudate, calculated from the SAXS profiles, was determined only by the function of T_e, independent of EDR and of morphology of predrawn films with different crystalline forms and different lamellar thickness. The higher the T_e, the longer the long period

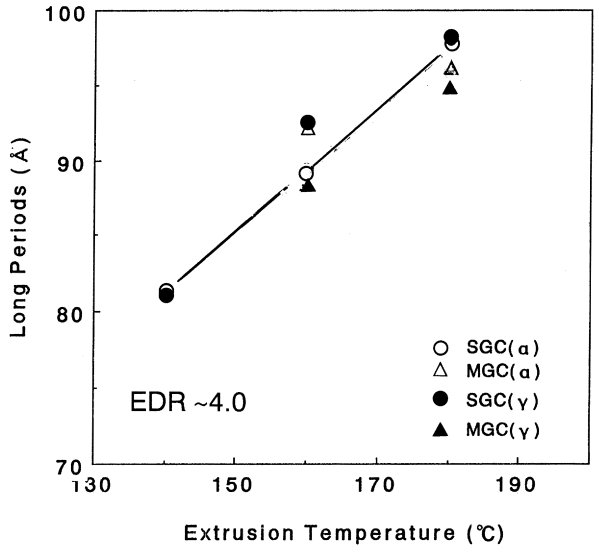

Figure 7 Relation between T_e and long period of the extrudates from the SGC and MGC films with α- and γ-forms (EDR~4.0)

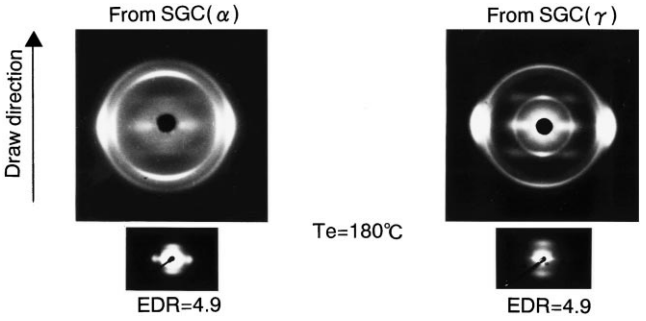

Figure 8 WAXD and SAXS photographs of the extrudates from $SGC_{(\alpha)}$ and $SGC_{(\gamma)}$

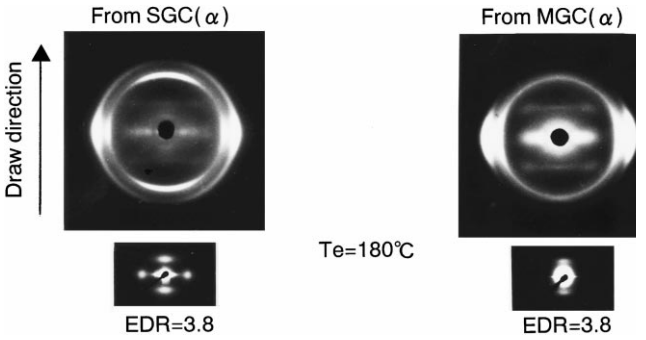

Figure 9 WAXD and SAXS photographs of the extrudates from $SGC_{(\alpha)}$ and $MGC_{(\alpha)}$

as shown in *Figure 7*. These results can be explained by the destruction of the original lamellae followed by a reorganization at T_e, similar to the case of polyethylene and polypropylene[27,28], and in accordance with the consideration by Arimoto[23].

The efficiency of draw in the crystalline regions was also affected by the initial crystalline form and the crystalline morphology. *Figure 8* shows the WAXD and SAXS photographs are shown for two extrudates with the same EDR of 4.9, but obtained from different crystalline forms, $SGC_{(\alpha)}$ and $SGC_{(\gamma)}$. For the $SGC_{(\alpha)}$, the crystal fiber axis oriented both parallel and perpendicular to the extrusion direction. In the SAXS pattern, the intensity maxima were observed on both meridian and equator. These results indicate that a part of the original lamellae was not deformed and stayed at the original position even after the extrusion[12]. On the other hand, for the $SGC_{(\gamma)}$, most of the crystal fiber axis oriented parallel to the extrusion direction and the intensity maxima from the original lamellae disappeared in the SAXS profile. *Figure 9* provides WAXD and SAXS photographs of two extrudates with the same EDR of 3.8, but obtained from different crystalline morphologies, $SGC_{(\alpha)}$ and $MGC_{(\alpha)}$. It can be clearly seen that the efficiency of draw, as evaluated by the chain orientation in the crystalline regions, is higher for the $MGC_{(\alpha)}$ than for the $SGC_{(\alpha)}$. It is well known that bulk crystallized morphology has many more intercrystalline tie molecules, compared with those in the solution-grown crystals. The present results suggest that the intercrystalline network plays an important role for the deformation of α-crystals of nylon-6. On the other hand, for the γ-crystals, the effects of intercrystalline networks on the efficiency of draw seem to be less prominent, because the WAXD and SAXS profiles of the extrudates from $SCC_{(\gamma)}$ are quite similar to those from $MGC_{(\gamma)}$, as revealed in *Figure 10*.

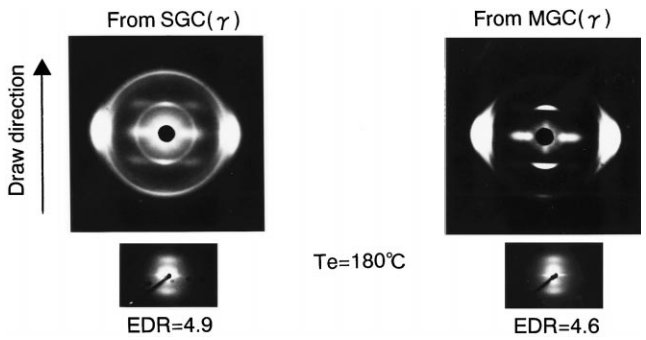

Figure 10 WAXD and SAXS photographs of the extrudates from $SGC_{(\gamma)}$ and $MGC_{(\gamma)}$

Kanamoto *et al*. reported[29] that the intercrystalline network and entanglements of the original samples of polyethylene have a remarkable effect on ductility, but do not have an important effect on the efficiency of draw. Further, they suggested that the interfacial friction and adhesion between crystalline lamellae is the primary mechanism for the deformation. In nylon-6 crystals, the chain sliding and/or slippage are severely restricted by the hydrogen bonding, which induces a high stress on draw. Thus, for nylon-6, the force of interfacial friction between lamellae is not large enough to pull out the chain from crystalline phases. In this case, the intercrystalline network is likely to play an important role in transmitting the stress on draw. Based on the crystallographic data[7,10,30,31] of the α- and γ-forms, the number of hydrogen bondings per volume and the distance between adjacent amidic groups in the crystalline regions were calculated. The numbers of the α- and γ-forms are 8.2×10^{-3} and 6.2×10^{-3} (per $Å^3$), respectively, and the distances for the α- and γ-forms are 1.6 and 2.1 Å, respectively.

Such differences might enhance the ductility as well as the efficiency of draw in the crystalline regions of nylon-6 with the γ-form.

CONCLUSION

(1) The crystalline form of solution-grown crystals of nylon-6 could be transformed from the α- to the γ-crystal form without a large scale molecular rearrangements.

(2) The deformability of nylon-6 was greatly affected by the crystalline form; the γ-form is more ductile than the α-form.

(3) However, the γ-type crystals were not completely deformed, even at the highest deformation ratio of 6.7 achieved in this work.

REFERENCES

1. Ciferri, A. and Ward, I. M., in *Ultra-High Modulus Polymers*. Applied Science, London, 1979.
2. Zachariades, A. E. and Porter, R. S., in *The Strength and Stiffness of Polymers*. Marcel Dekker, New York, 1983.
3. Zachariades, A. E. and Porter, R. S., in *High Modulus Polymers: Approaches to Design and Developments*. Marcel Dekker, New York, 1988.
4. Lemstra, P. J. and Kleintjens, L. A., in *Integration of Fundamental Polymer Science and Technology—3*. Elsevier Applied Science, London, 1989.
5. Huang, B., Ito, M. and Kanamoto, T., *Polymer*, 1994, **35**, 1210.
6. Lin, A. and Argon, A.S., *Macromolecules*, 1992, **25**, 4011.
7. Holes, D. R., Bunn, C. W. and Smith, D. J., *J. Polym. Sci.*, 1955, **17**, 159.
8. Arimoto, H., Ishibashi, M. and Chatani, Y., *J. Polym. Sci., Part A*, 1965, **3**, 317.
9. Vogelsong, D. C., *J. Polym. Sci. A*, 1963, **1**, 1055.
10. Arimoto, H., *J. Polym. Sci., A*, 1964, **2**, 2283.
11. Wunderlich, B., in *Macromolecular Physics*, Vol. 1. Academic Press, New York, 1973, p. 389.
12. Ito, M., Morishita, Y., Mizuochi, K. and Kanamoto, T., *J. Macromol. Sci-Phys.*, 1997, **B36**, (3), 367.
13. Chuah, H. H. and Porter, R. S., *Polymer*, 1986, **27**, 241.
14. Murthy, N. S., *Macromolecules*, 1987, **20**, 309.
15. Murthy, N. S., *Macromolecules*, 1990, **23**, 1342.
16. Kawaguchi, A., *Polymer*, 1992, **33**, 3981.
17. Lee, Y. H. and Porter, R. S., *J. Macromol. Sci.-Phys.*, 1995, **B34**, 295.
18. Tashiro, K. and Tadokoro, H., *Macromolecules*, 1981, **14**, 781.
19. McCrum, N. G., Read, B. F. and Williams, G., in *Anelastic and Dielectric Effects in Polymer Solids*. Wiley, New York, 1967.
20. Frayer, P. D., Koenig, J. and Lando, J. B., *J. Macromol. Sci.-Phys.*, 1972, **B6**, 129.
21. Matsubara, I. and Magill, J. H., *Polymer*, 1966, **7**, 199.
22. Abu-Isa, I., *J. Polym. Sci., A-1*, 1971, **9**, 199.
23. Arimoto, H., *Kobunshi Kagaku*, 1962, **19**, 212.
24. Miyasaka, K. and Ishikawa, K., *J. Polym. Sci., A-1*, 1967, **5**, 3017.
25. Miyasaka, K. and Ishikawa, K., *J. Polym. Sci., A2*, 1968, **6**, 1317.
26. Murthy, N. S., Bray, R. G., Correale, S. T. and Moore, R. A. F., *Polymer*, 1995, **36**, 3863.
27. Corneliussen, R. and Peterlin, A., *Makromol. Chem.*, 1967, **105**, 193.
28. Balta-Calleija, F. J. and Peterlin, A., *J. Mater. Sci.*, 1969, **4**, 799.
29. Kanamoto, T., Sherman, E. S. and Porter, R. S., *Polymer J.*, 1979, **11**, 497.
30. Kinoshita, Y., *Makromol. Chem.*, 1959, **33**, 21.
31. Paker, J. P. and Lindenmeyer, P. H., *J. Appl. Polym. Sci.*, 1977, **21**, 821.